Wave–particle duality of C_{60} molecules

Markus Arndt, Olaf Nairz, Julian Vos-Andreae, Claudia Keller, Gerbrand van der Zouw & Anton Zeilinger

Institut für Experimentalphysik, Universität Wien, Boltzmanngasse 5, A-1090 Wien, Austria

Quantum superposition lies at the heart of quantum mechanics and gives rise to many of its paradoxes. Superposition of de Broglie matter waves[1] has been observed for massive particles such as electrons[2], atoms and dimers[3], small van der Waals clusters[4], and neutrons[5]. But matter wave interferometry with larger objects has remained experimentally challenging, despite the development of powerful atom interferometric techniques for experiments in fundamental quantum mechanics, metrology and lithography[6]. Here we report the observation of de Broglie wave interference of C_{60} molecules by diffraction at a material absorption grating. This molecule is the most massive and complex object in which wave behaviour has been observed. Of particular interest is the fact that C_{60} is almost a classical body, because of its many excited internal degrees of freedom and their possible couplings to the environment. Such couplings are essential for the appearance of decoherence[7,8], suggesting that interference experiments with large molecules should facilitate detailed studies of this process.

When considering de Broglie wave phenomena of larger and more complex objects than atoms, fullerenes come to mind as suitable candidates. After their discovery[9] and the subsequent invention of efficient mass-production methods[10], they became easily available. In our experiment (see Fig. 1) we use commercial, 99.5% pure, C_{60} fullerenes (Dynamic Enterprises Ltd, Twyford, UK) which were sublimated in an oven at temperatures between 900 and 1,000 K. The emerging molecular beam passed through two collimation slits, each about 10 μm wide, separated by a distance of 1.04 m. Then it traversed a free-standing nanofabricated SiN_x grating[11] consisting of nominally 50-nm-wide slits with a 100-nm period.

At a further distance of 1.25 m behind the diffraction grating, the interference pattern was observed using a spatially resolving detector. It consisted of a beam from a visible argon-ion laser (24 W all lines), focused to a gaussian waist of 8 μm width (this is the size required for the light intensity to drop to $1/e^2$ of that in the centre of the beam). The light beam was directed vertically, parallel both to the lines of the diffraction grating and to the collimation slits. By using a suitable mirror assembly, the focus could be scanned with micrometre resolution across the interference pattern. The absorbed light then ionized the C_{60} fullerenes via heating and subsequent thermal emission of electrons[12]. The detection region was found to be smaller than 1 mm in height, consistent with a full Rayleigh length of 800 μm and the strong power dependence of this ionization process. A significant advantage of the thermionic mechanism is that it does not detect any of the residual gases present in the vacuum chamber. We could thus achieve dark count rates of less than one per second even under moderately high vacuum conditions (5×10^{-7} mbar). The fullerene ions were then focused by an optimized ion lens system, and accelerated to a BeCu conversion electrode at −9 kV where they induced the emission of electrons which were subsequently amplified by a Channeltron detector.

Alignment is a crucial part of this experiment. In order to be able to find the beam in the first place, our collimation apertures are movable piezo slits that can be opened from 0 to 60 μm (in the case of the first slit) and from 0 to 200 μm (for the second slit). The vacuum chamber is rigidly mounted on an optical table together with the ionizing laser, in order to minimize spatial drifts.

The effect of gravity also had to be considered in our set-up. For the most probable velocity (220 m s^{-1}), the fullerenes fall by 0.7 mm while traversing the apparatus. This imposes a constraint on the maximum tilt that the grating may have with respect to gravity. As a typical diffraction angle into the first-order maximum is 25 μrad, one can tolerate a tilt angle of (at most) about one mrad before molecules start falling from one diffraction order into the trajectory of a neighbouring order of a different velocity class. The experimental curves start to become asymmetric as soon as the grating tilt deviates by more than 500 μrad from its optimum vertical orientation.

The interference pattern of Fig. 2a clearly exhibits the central maximum and the first-order diffraction peaks. The minima between zeroth and first orders are well developed, and are due to destructive interference of C_{60} de Broglie waves passing through neighbouring slits of the grating. For comparison, we show in Fig. 2b the profile of the undiffracted collimated beam. The velocity distribution has been measured independently by a time-of-flight method; it can be well fitted by $f(v) = v^3 \exp(-(v - v_0)^2/v_m^2)$, with $v_0 = 166\,\mathrm{m\,s^{-1}}$ and $v_m = 92\,\mathrm{m\,s^{-1}}$ as expected for a transition between a maxwellian effusive beam and a supersonic beam[13]. The most probable velocity was $v = 220\,\mathrm{m\,s^{-1}}$, corresponding to a de Broglie wavelength of 2.5 pm. The full-width at half-maximum was as broad as 60%, resulting in a longitudinal coherence length of about 5 pm.

The essential features of the interference pattern can be understood using standard Kirchhoff diffraction theory[14] for a grating with a period of 100 nm, by taking into account both the finite width of the collimation and the experimentally determined velocity distribution. The parameters in the fit were the width of the collimation, the gap width s_0 of a single slit opening, the effective beam width of the detection laser and an overall scaling factor. This model, assuming all grating slits to be perfect and identical, reproduces very well the central peak of the interference pattern shown in Fig. 2a, but does not fit the 'wings' of this pattern.

Agreement with the experimental data, including the 'wings' in

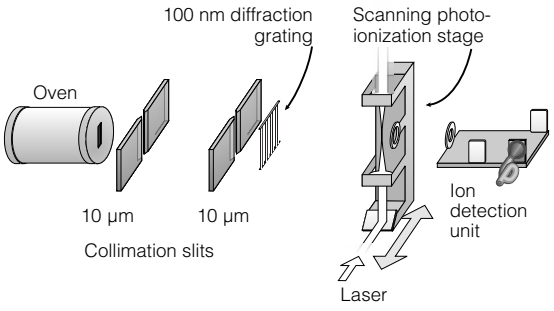

Figure 1 Diagram of the experimental set-up (not to scale). Hot, neutral C_{60} molecules leave the oven through a nozzle of 0.33 mm × 1.3 mm × 0.25 mm (width × height × depth), pass through two collimating slits of 0.01 mm × 5 mm (width × height) separated by 1.04 m, traverse a SiN_x grating (period 100 nm) 0.1 m after the second slit, and are detected via thermal ionization by a laser 1.25 m behind the grating. The ions are then accelerated and directed towards a conversion electrode. The ejected electrons are subsequently counted by a Channeltron electron multiplier. The laser focus can be reproducibly scanned transversely to the beam with 1-μm resolution.

Fig. 2a, can be achieved by allowing for a gaussian variation of the slit widths over the grating, with a mean open gap width centred at $s_0 = 38$ nm with a full-width at half-maximum of 18 nm. That best-fit value for the most probable open gap width s_0 is significantly smaller than the 55 ± 5 nm specified by the manufacturer (T. A. Savas and H. Smith, personal communication). This trend is consistent with results obtained in the diffraction of noble gases and He clusters, where the apparently narrower slit was interpreted as being due to the influence of the van der Waals interaction with the SiN_x grating during the passage of the molecules[15]. This effect is expected to be even more pronounced for C_{60} molecules owing to their larger polarizability. The width of the distribution seems also justified in the light of previous experiments with similar gratings: both the manufacturing process and adsorbents could account for this fact (ref. 16, and T. A. Savras and H. Smith, personal communication). Recently, we also observed interference of C_{70} molecules.

Observation of quantum interference with fullerenes is interesting for various reasons. First, the agreement between our measured and calculated interference contrast suggests that not only the highly symmetric, isotopically pure $^{12}C_{60}$ molecules contribute to the interference pattern but also the less symmetric isotopomeric variants $^{12}C_{59}{}^{13}C$ and $^{12}C_{58}{}^{13}C_2$ which occur with a total natural abundance of about 50%. If only the isotopically pure $^{12}C_{60}$ molecules contributed to the interference, we would observe a much larger background.

Second, we emphasize that for calculating the de Broglie wavelength, $\lambda = h/Mv$, we have to use the complete mass M of the object. Thus, each C_{60} molecule acts as a whole undivided particle during its centre-of-mass propagation.

Last, the rather high temperature of the C_{60} molecules implies broad distributions, both of their kinetic energy and of their internal energies. Our good quantitative agreement between experiment and theory indicates that the latter do not influence the observed coherence. All these observations support the view that each C_{60} molecule interferes with itself only.

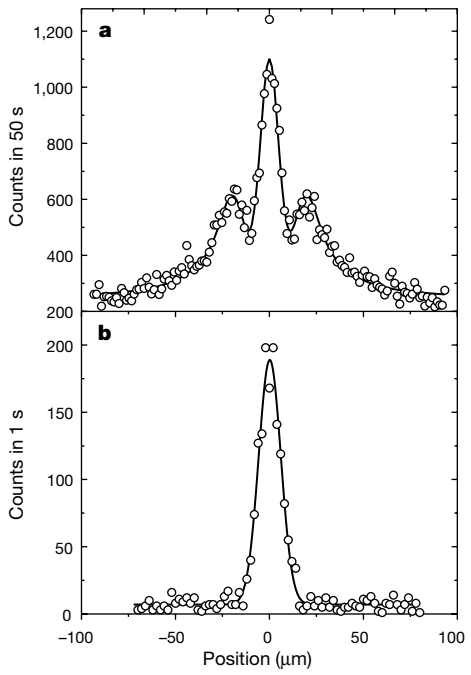

Figure 2 Interference pattern produced by C_{60} molecules. **a**, Experimental recording (open circles) and fit using Kirchhoff diffraction theory (continuous line). The expected zeroth and first-order maxima can be clearly seen. Details of the theory are discussed in the text. **b**, The molecular beam profile without the grating in the path of the molecules.

In quantum interference experiments, coherent superposition only arises if no information whatsoever can be obtained, even in principle, about which path the interfering particle took. Interaction with the environment could therefore lead to decoherence. We now analyse why decoherence has not occurred in our experiment and how modifications of our experiment could allow studies of decoherence using the rich internal structure of fullerenes.

In an experiment of the kind reported here, 'which-path' information could be given by the molecules in scattering or emission processes, resulting in entanglement with the environment and a loss of interference. Among all possible processes, the following are the most relevant: decay of vibrational excitations via emission of infrared radiation, emission or absorption of thermal blackbody radiation over a continuous spectrum, Rayleigh scattering, and collisions.

When considering these effects, one should keep in mind that only those scattering processes which allow us to determine the path of a C_{60} molecule will completely destroy in a single event the interference between paths through neighbouring slits. This requires $\lambda \ll d$; that is, the wavelength λ of the incident or emitted radiation has to be smaller than the distance d between neighbouring slits, which amounts to 100 nm in our experiment. When this condition is not fulfilled decoherence is however also possible via multi-photon scattering[7,8,17].

At $T \approx 900$ K, as in our experiment, each C_{60} molecule has on average a total vibrational energy of $E_v \approx 7$ eV (ref. 18) stored in 174 vibrational modes, four of which may emit infrared radiation at $\lambda_{vib} \approx 7$–19 μm (ref. 10) each with an Einstein coefficient of $A_k \approx 100\,s^{-1}$ (ref. 18). During its time of flight from the grating towards the detector ($\tau \approx 6$ ms) a C_{60} molecule may thus emit on average 2–3 such photons.

In addition, hot C_{60} has been observed[19] to emit continuous blackbody radiation, in agreement with Planck's law, with a measured integrated emissivity of $\epsilon \approx 4.5\ (\pm 2.0) \times 10^{-5}$ (ref. 18). For a typical value of $T \approx 900$ K, the average energy emitted during the time of flight can then be estimated as only $E_{bb} \approx 0.1$ eV. This corresponds to the emission of (for example) a single photon at $\lambda \approx 10$ μm. Absorption of blackbody radiation has an even smaller influence as the environment is at a lower temperature than the molecule. Finally, since the mean free path for neutral C_{60} exceeds 100 m in our experiment, collisions with background molecules can be neglected.

As shown above, the wavelengths involved are too large for single photon decoherence. Also, the scattering rates are far too small to induce sufficient phase diffusion. This explains the decoupling of internal and external degrees of freedom, and the persistence of interference in our present experiment.

A variety of unusual decoherence experiments would be possible in a future extension of the experiment, using a large-area interferometer. A three-grating Mach–Zehnder interferometer[6] seems to be a particularly favourable choice, since for a grating separation of up to 1 m we will have a molecular beam separation of up to 30 μm, much larger than the wavelength of a typical thermal photon. In this case, the environment obtains 'which-path' information even through a single thermal photon, and the interference contrast should thus be completely destroyed. The parameters that could be controlled continuously in such an experiment would then be the internal temperature of the fullerenes, the temperature of the environment, the intensity and frequency of external laser radiation, the interferometer size, and the background pressure of various gases.

An improved interferometer could have other applications. For example, in contrast to previous atom-optical experiments[20–22] which were limited to the interaction with only a few lines in the whole spectrum, interferometry with fullerenes would enable us to study these naturally occurring and ubiquitous thermal processes and wavelength-dependent decoherence mechanisms for (we

believe) the first time. Another possible application of molecule interferometry is precision metrology; the improved interferometer could be used to measure molecular polarizabilities[6]. Moreover, it might be possible to nanofabricate SiC patterns on Si substrates using C_{60} interferometry.

Furthermore, we note the fundamental difference between isotopically pure C_{60}, which should exhibit bosonic statistics, and the isotopomers containing one ^{13}C nucleus, which should exhibit fermionic statistics. We intend to explore the possibility of observing this feature, for example by showing the different rotational symmetry between the two species in an interferometer[23,24].

In our experiment, the de Broglie wavelength of the interfering fullerenes is already smaller than their diameter by a factor of almost 400. It would certainly be interesting to investigate the interference of objects the size of which is equal to or even bigger than the diffracting structure. Methods analogous to those used for the present work, probably extended to the use of optical diffraction structures, could also be applied to study quantum interference of even larger macromolecules or clusters, up to small viruses[25,26]. □

Received 30 June; accepted 2 September 1999.

1. de Broglie, L. Waves and quanta. *Nature* **112,** 540 (1923).
2. Davisson, C. J. & Germer, L. H. The scattering of electrons by a single crystal of nickel. *Nature* **119,** 558–560 (1927).
3. Estermann, I. & Stern, O. Beugung von Molekularstrahlen. *Z. Phys.* **61,** 95–125 (1930).
4. Schöllkopf, W. & Toennies, J. P. Nondestructive mass selection of small van der Waals clusters. *Science* **266,** 1345–1348 (1994).
5. Halban, H. v. Jr & Preiswerk, P. Preuve expérimentale de la diffraction des neutrons. *C.R. Acad. Sci.* **203,** 73–75 (1936).
6. Berman, P. (ed.) *Atom Interferometry* (Academic, 1997).
7. Zurek, W. H. Decoherence and the transition from quantum to classical. *Phys. Today* 36–44 (October 1991).
8. Giulini, D. *et al. Decoherence and the Appearance of the Classical World in Quantum Theory* (Springer, Berlin, 1996).
9. Kroto, H. W., Heath, J. R., O'Brien, S. C., Curl, R. F. & Smalley, R. E. C_{60}: buckminsterfullerene. *Nature* **318,** 162–166 (1985).
10. Krätschmer, W., Lamb, L. D., Fostiropoulos, K. & Huffman, D. R. A new form of carbon. *Nature* **347,** 354–358 (1990).
11. Savas, T. A., Shah, S. N., Schattenburg, M. L., Carter, J. M. & Smith, H. I. Achromatic interferometric lithography for 100-nm-period gratings and grids. *J. Vac. Sci. Technol. B* **13,** 2732–2735 (1995).
12. Ding, D., Huang, J., Compton, R. N., Klots, C. E. & Haufler, R. E. cw laser ionization of C_{60} and C_{70}. *Phys. Rev. Lett.* **73,** 1084–1087 (1994).
13. Scoles, G. (ed.) *Atomic and Molecular Beam Methods* Vol. 1 (Oxford Univ. Press, 1988).
14. Born, M. & Wolf, E. *Principles of Optics* (Pergamon, Oxford, 1984).
15. Grisenti, R. E., Schöllkopf, W., Toennies, J. P., Hegerfeldt, G. C. & Köhler, T. Determination of atom-surface van der Waals potentials from transmission-grating diffraction intensities. *Phys. Rev. Lett.* **83,** 1755–1758 (1999).
16. Grisenti, R. E. *et al.* He atom diffraction from nanostructure transmission gratings: the role of imperfections. *Phys. Rev. A* (submitted).
17. Joos, E. & Zeh, H. D. The emergence of classical properties through interaction with the environment. *Z. Phys. B.* **59,** 223–243 (1985).
18. Kolodney, E., Budrevich, A. & Tsipinyuk, B. Unimolecular rate constants and cooling mechanisms of superhot C_{60} molecules. *Phys. Rev. Lett.* **74,** 510–513 (1995).
19. Mitzner, R. & Campbell, E. E. B. Optical emission studies of laser desorbed C_{60}. *J. Chem. Phys.* **103,** 2445–2453 (1995).
20. Pfau, T., Spälter, S., Kurtsiefer, Ch., Ekstrom, C. R. & Mlynek, J. Loss of spatial coherence by a single spontaneous emission. *Phys. Rev. Lett.* **73,** 1223–1226 (1994).
21. Clauser, J. F. & Li, S. "Heisenberg microscope" decoherence atom interferometry. *Phys. Rev. A* **50,** 2430–2433 (1994).
22. Chapman, M. S. *et al.* Photon scattering from atoms in an atom interferometer: Coherence lost and regained. *Phys. Rev. Lett.* **75,** 3783–3787 (1995).
23. Werner, S. A., Colella, R., Overhauser, A. W. & Eagen, C. F. Observation of the phase shift of a neutron due to precession in a magnetic field. *Phys. Rev. Lett.* **35,** 1053–1055 (1975).
24. Rauch, H. *et al.* Verification of coherent spinor rotation of fermions. *Phys. Lett. A* **54,** 425–427 (1975).
25. Clauser, J. F. in *Experimental Metaphysics* (eds Cohen, R. S., Home, M. & Stachel, J.) 1–11 (Kluwer Academic, Dordrecht, 1997).
26. Arndt, M., Nairz, O., van der Zouw, G. & Zeilinger, A. in *Epistemological and Experimental Perspectives on Quantum, Physics* (eds Greenberger, D., Reiter, W. L. & Zeilinger, A.) 221–224 (IVC Yearbook, Kluwer Academic, Dordrecht, 1999).

Acknowledgements

We thank M. Haluška, H. Kuzmany, R. Penrose, P. Scheier, J. Schmiedmayer and G. Senn for discussions. This work was supported by the Austrian Science Foundation FWF, the Austrian Academy of Sciences, the TMR programme of the European Union, and the US NSF.

Correspondence and requests for materials should be addressed to A.Z. (e-mail: zeilinger-office@exp.univie.ac.at).

Lanthanum-substituted bismuth titanate for use in non-volatile memories

B. H.Park*, B. S. Kang*, S. D. Bu*, T. W. Noh*, J. Lee† & W. Jo‡

** Department of Physics and Condensed Matter Research Institute, Seoul National University, Seoul 151-742, Korea*
† Department of Materials Engineering, Sung Kyun Kwan University, Suwon 440-746, Korea
‡ LG Corporate Institute of Technology, Seoul 137-140, Korea

Non-volatile memory devices are so named because they retain information when power is interrupted; thus they are important computer components. In this context, there has been considerable recent interest[1,2] in developing non-volatile memories that use ferroelectric thin films—'ferroelectric random access memories', or FRAMs—in which information is stored in the polarization state of the ferroelectric material. To realize a practical FRAM, the thin films should satisfy the following criteria: compatibility with existing dynamic random access memory technologies, large remnant polarization (P_r) and reliable polarization-cycling characteristics. Early work focused on lead zirconate titanate (PZT) but, when films of this material were grown on metal electrodes, they generally suffered from a reduction of P_r ('fatigue') with polarity switching. Strontium bismuth tantalate (SBT) and related oxides have been proposed to overcome the fatigue problem[3], but such materials have other shortcomings, such as a high deposition temperature. Here we show that lanthanum-substituted bismuth titanate thin films provide a promising alternative for FRAM applications. The films are fatigue-free on metal electrodes, they can be deposited at temperatures of ~650 °C and their values of P_r are larger than those of the SBT films.

The structure of FRAM is very similar to that of conventional dynamic random access memory (DRAM), where memory cells are arranged in a square matrix. (Therefore, FRAM should, in principle, have a lower power requirement, a faster access time and a potentially lower cost than many other non-volatile memory devices[1,3].) A DRAM cell usually has a capacitor, where the binary information will be stored in terms of the signs of the stored charge. To maintain this information, a voltage should be continually applied to compensate for charge reduction due to leakage currents. In FRAM, the dielectric material in the capacitor is replaced with a ferroelectric film. Then, information can be stored in the polarization states of the ferroelectric thin film: that is, two spontaneous polarization states under zero electric field can be utilized as '0' and '1' digital states. It seems that the first generation of FRAM will be based on a destructive reading scheme, where a bit is read when a positive switching voltage (that is, an applied electric field) is applied to the memory cell[2]. If the cell polarization is already along the same direction, then only a linear non-switching response, P_{ns}, is measured. If it is in the opposite direction, a switching response, P_{sw}, is measured. Therefore $(P_{sw} - P_{ns})$, which should be nearly the same as $2P_r$, is an important quantity which determines the performance of FRAM. It should be large enough for signal detection and should not change under repetitive read/write cycles.

The PZT and other related ferroelectric films, which are most widely investigated, usually have large values of $(P_{sw} - P_{ns})$: depending on substituting elements and processing conditions, reported values vary from 20 to 70 $\mu C\,cm^{-2}$ (refs 4, 5). However, when a capacitor is fabricated with the PZT film on conventional platinum (Pt) electrodes, its value of $(P_{sw} - P_{ns})$ is usually reduced after repetitive read/write cycles. This fatigue problem might be induced